IJMOT

INTERNATIONAL JOURNAL OF MICROWAVE AND OPTICAL TECHNOLOGY,

VOL.6, NO.2, MARCH 2011

Hybrid Neural Network/Modal Method Modeling of Uniaxial Waveguide Discontinuities

M. Yahia*[+#¤], J. W. Tao[¤2], H. Benzina[#3], M. N. Abdelkrim[+#4]

[+]Unité de Recherche Modélisation, Analyse et Commande des Systèmes MACS
[#]Ecole Nationale d'Ingénieurs de Gabès Rue Omar Ibn Elkhattab 6029 Gabès Tunisia
*Tel: 00-216-96-171-889; Fax: 00-216-75-392-190; E-mail: mohamed_yahia1@yahoo.fr
hafed.benzina@enig.rnu.tn
naceur.abdelkrim@enig.rnu.tn
[¤]Laboratoire Plasma et Conversion d'Energie LAPLACE
Ecole Nationale Supérieure d'Electrotechnique, d'Electronique, d'Informatique, d'Hydraulique et des Télécommunications, 2 rue Camichel 31071 Toulouse cedex France
tao@laplace.univ-tls.fr

***Abstract*-We propose a hybrid neural network/modal method computer-aided design (CAD) tool to the analysis of uniaxial discontinuities in rectangular waveguides. The neural network is trained using the continuity conditions of the transverse electric and magnetic fields in the discontinuity plane. Unlike the conventional modal methods, the performances of the proposed neuromodel are controlled by the operator and can outperform the classical modal methods in CPU time. The parallel nature of the proposed hybrid CAD tool makes it an interesting solution for parallel implementation in hardware and software.**

***Index Terms*- Uniaxial discontinuities, modal methods, artificial neural networks, hybrid methods.** [1]

I. INTRODUCTION

The artificial neural networks (ANNs) are information processing tools inspired by the ability of the human brain to learn and to generalize by abstraction [1]. After the training, the ANNs produce accurate and instantaneous responses. Consequently, they are applied in diverse scientific fields (image processing, speech processing, medical, robot, pattern recognition…). Their use in electromagnetic is in expansion especially in microwave circuits [2].

The uniaxial discontinuities in waveguides are widely utilized for the design of numerous passive microwave components for spatial applications (e.g., filters, diplexers and multiplexers, polarizers, etc). In [3], authors proposed a hybrid finite element method (FEM) and ANNs CAD tool to solve second order partial derivative problems. The weights of the ANNs are trained with the nodal finite element system equations. They successfully applied their neuromodel to the analysis of numerous waveguide configurations. Also, the similar CAD tools that combine FEM and ANNs are given in [4–7]. In [8], the solutions to electromagnetic compatibility problems are given by combining vector finite element method with ANNs.

However, when considering simple discontinuities in waveguides, the modal method (e. g. multimodal variational method (MVM) [9], the mode matching (MM) [10], etc.) are the most appropriate CAD tools used for such devices. They outperform spatial meshing technique (i. e.

M. Yahia et al , "Uniaxial Discontinuities Analysis Using the Artificial Neural Networks ", *International Conference on Signals, Circuits and Systems*, 6-8 Nov. 2009, Djerba.

INTERNATIONAL JOURNAL OF MICROWAVE AND OPTICAL TECHNOLOGY,
VOL.6, NO.2, MARCH 2011

finite element [11] and finite difference [12]) in CPU time and memory storage.

In this paper, we substitute the finite element formulation in [3-8] by the modal one. The ANN is trained using the continuity conditions of the transverse electric and magnetic fields in the discontinuity plane. The neuromodel is applied to the analysis of well-known discontinuities. All simulations are developed in Matlab on a PC (Intel CPU 1.66 GHz with 1-GB RAM).

II. UNIAXIAL WAVEGUIDE DISCONTINUITIES

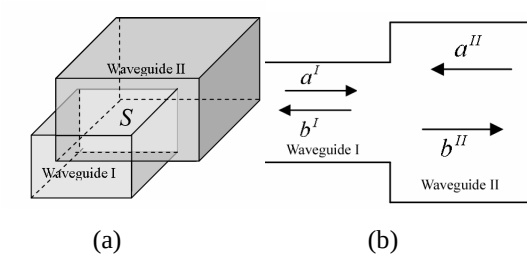

(a) (b)

Fig. 1. Uniaxial discontinuity between two rectangular waveguides.

Fig.1. presents a uniaxial discontinuity between two rectangular waveguides. In the *S* discontinuity surface, the continuity conditions of the transverse electric and magnetic fields can be expressed as follows:

$$\zeta_1 = \sum_{m=1}^{N1} A_m^I \left(a_m^I + b_m^I\right) e_m^I - \sum_{p=1}^{N2} A_p^{II} \left(a_p^{II} + b_p^{II}\right) e_p^{II} = 0 \quad (1)$$

$$\zeta_2 = \sum_{m=1}^{N1} B_m^I \left(a_m^I - b_m^I\right) h_m^I - \sum_{p=1}^{N2} B_p^{II} \left(-a_p^{II} + b_p^{II}\right) h_p^{II} = 0 \quad (2)$$

N_1 and N_2 are the numbers of modes in the waveguides I and II, respectively. a_m^i and b_m^i being the incident and reflected wave amplitudes of the m[th] eigenmode at the discontinuity plane in th i[th] waveguide, respectively. e_m^i and h_m^i being the m[th] modal electric and magnetic basis functions in the i[th] waveguide, respectively. A_m^i and B_m^i are two complex parameters where the ratio A_m^i / B_m^i being the modal impedance.

III. THE PROPOSED NEUROMODEL

A. General Architecture of the ANNs

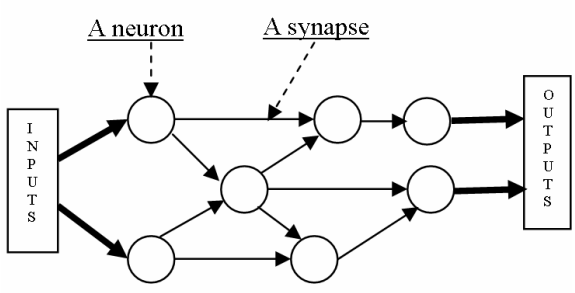

Fig. 2. Architecture of the ANNs

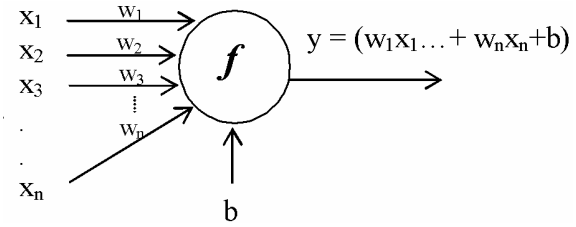

Fig. 3. Structure of a neuron

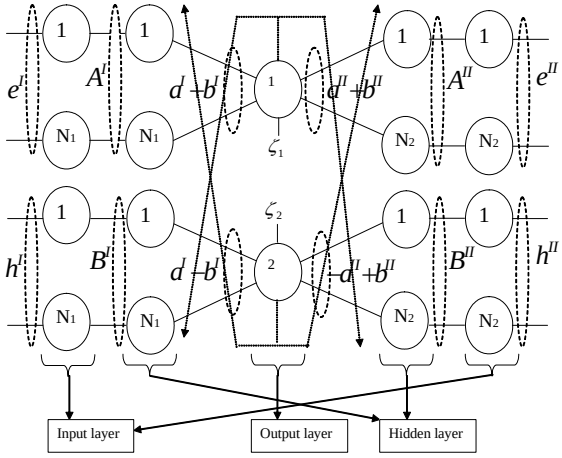

Fig. 4. The proposed neuromodel architecture.

Generally, ANNs have two components:

- The processing elements called neurons (fig. 2).

- The connections between neurons are called *links* or *synapses*. Each link has a weight coefficient (w_i) (fig. 2).

Each neuron receives inputs (stimuli x_i) from neighboring neurons connected to it, process the information (*f*) and generate an output (y) (fig. 3). Neurons that receive stimuli from outside the ANN constitute the input layer. Neurons whose outputs are used outside the ANN form the output layer. Neurons whose inputs and outputs are in the ANN constitute the hidden layer. There are different kinds of ANNs. In this paper, we are interested in the multilayer perceptron neural network (MLPNN) [1].

B. Application of the hybrid CAD Tool to the Analysis of Waveguide Discontinuities.

Equations (1) and (2) can be expressed in a MLPNN model (fig. 4) where *f* is the identity function and b is equal to zero (fig. 3). The architecture of the neuromodel is detailed as follows:

- Input layer: the number of neurons in the input layer is equal to N_1+N_2.
- Hidden layer: the number of neurons in the hidden layer is equal to the one in the input layer.
- Output layer: we take two neurons which generate ζ_1 and ζ_2.

The waveguide I is excited by the fundamental mode TE_{10}. Consequently, $a^{II}=0$ and $a^{I}=0$ except $a^{I}(1)=1$. In fig. 4, the unknowns are b^I and b^{II}. They will be computed iteratively in the training process. To get a solution to the equations (1) and (2), the outputs of the proposed neuromodel must generate $\zeta_1=0$ and $\zeta_2=0$. To attain this end, we employ the least mean squares (LMS) algorithm [13]. We minimize simultaneously $|\zeta_1|^2$ and $|\zeta_2|^2$. The parameters b^I and b^{II} are adjusted using the following iterative expressions:

$$b^{II}=b^{II}-\mu^*\nabla_{b^{II}}\left(|\zeta_1|^2\right) \tag{3}$$

$$b^{I}=b^{I}-\mu^*\nabla_{b^{I}}\left(|\zeta_2|^2\right) \tag{4}$$

* being the complex conjugate, ∇ is the gradient operator and μ being the step parameter where $0<\mu<1$.

$$\nabla_{b_k^I}\left(|\zeta_2|^2\right)=-2\zeta_2\frac{d\,\zeta_2^*}{d\,b_k^I}=-2\,\zeta_2 B_k^{I*}h_k^I \tag{5}$$
$$=2\left(-|B_k^I|^2\left(a_k^I-b_k^I\right)+\sum_{p=1}^{N2}B_p^{II}B_k^{I*}\left(-a_p^{II}+b_p^{II}\right)\langle h_p^{II}|h_k^I\rangle\right)$$

$$b_k^I=b_k^I-2\mu\left(-|B_k^I|^2\left(a_k^I-b_k^I\right)+\sum_{p=1}^{N2}B_p^{II}B_k^{I*}\left(-a_p^{II}+b_p^{II}\right)\langle h_p^{II}|h_k^I\rangle\right) \tag{6}$$

$$\nabla_{b_k^{II}}\left(|\zeta_1|^2\right)=-2\zeta_1\frac{d\,\zeta_1^*}{d\,b_k^{II}}=-2\zeta_1 A_k^{II*}e_k^{II} \tag{7}$$
$$=2\sum_{p=1}^{N1}-A_p^IA_k^{II*}\left(a_p^I+b_p^I\right)\langle e_p^I|e_k^{II}\rangle+2|A_k^{II}|^2\left(a_k^{II}+b_k^{II}\right)$$

$$b_k^{II}=b_k^{II}-2\mu\left(-\sum_{p=1}^{N1}A_p^IA_k^{II*}\left(a_p^I+b_p^I\right)\langle e_p^I|e_k^{II}\rangle+|A_k^{II}|^2\left(a_k^{II}+b_k^{II}\right)\right) \tag{8}$$

$\langle .|. \rangle$ being the inner product defined as follows.

$$\left\langle e_p^I(x,y)\middle|e_k^{II}(x,y)\right\rangle=\int_{x,y\in S}e_p^I(x,y)^*e_k^{II}(x,y)\,dxdy \tag{9}$$

The training process progresses as follows:

i. Compute the inner product between modes, choose the value of μ, initialize randomly b^I and b^{II} and choose a convergence threshold ψ.

ii. Adjust b^I and b^{II} using the expressions (6) and (8). Compute the relative error η between two successive iterations n and n+1 as:

$$\eta=\left|\left[\left(b^{I^{n+1}}-b^{I^n}\right)\left(b^{II^{n+1}}-b^{II^n}\right)\right]\right|\times100\Big/\left|\left[b^{I^{n+1}}\,b^{II^{n+1}}\right]\right| \tag{10}$$

iii. Repeat step ii while $\eta\geq\psi$.

iv. Compute the reflection and the transmission coefficients of the discontinuity which are expressed as follows.

$$S_{11} = b^I(1) / a^I(1) = b^I(1) \quad (11)$$

$$S_{12} = b^{II}(1) / a^I(1) = b^{II}(1) \quad (12)$$

IV. RESULTS

In this section, we apply the hybrid model to the analysis of various discontinuities in rectangular waveguides. The performances are compared to various modal methods. The modes in the waveguides in both side of the discontinuity are ordered by ascendant cut-off frequencies.

A. E-H Discontinuity

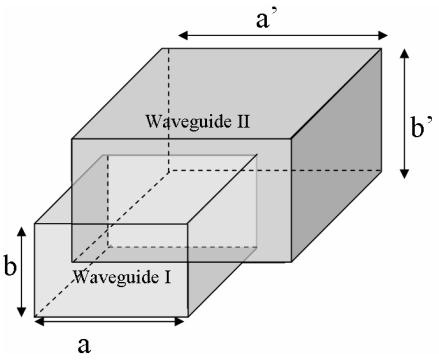

Fig. 5. E-H Discontinuity.

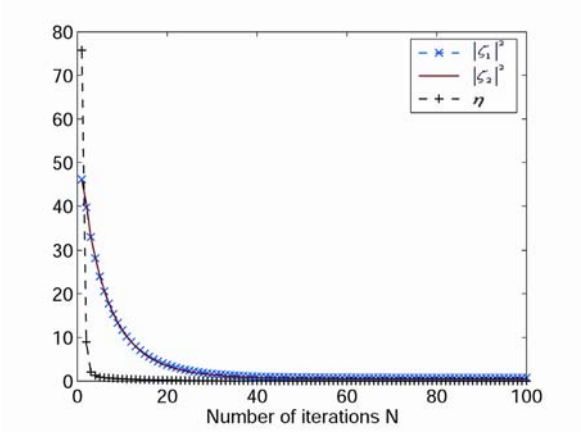

Fig. 6. Variation of η, $|\zeta_1|^2$ and $|\zeta_2|^2$ according to the number of iterations N for f =11.5 GHz and μ=0.055.

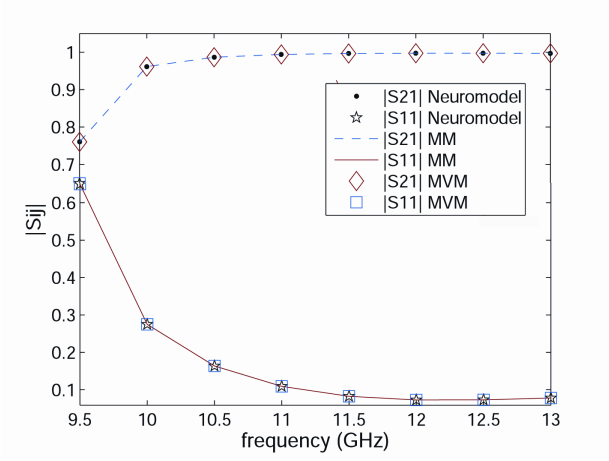

Fig. 7. $|S_{11}|$ and $|S_{12}|$ of the studied numerical methods for the E-H discontinuity.

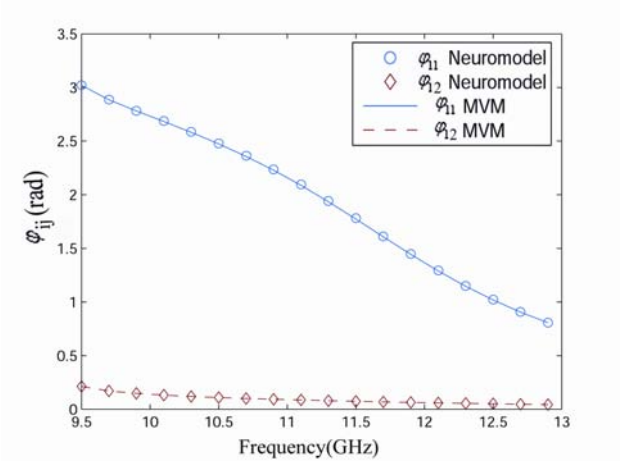

Fig. 8. Phases of the S paramerers of the studied numerical methods for the E-H discontinuity.

Table 1: CPU time of the studied numerical methods for the E-H discontinuity

	MM	MVM	Proposed Neuromodel
CPU time (s)	5.06	4.96	4.70

We consider an E-H discontinuity between a WR62 waveguide (a=15.799 mm, b=7.899 mm) and a WR90 waveguide (a'=22.86 mm, b'=10.16 mm) (fig. 5). We take 50 modes in the waveguide I and 96 modes in the waveguide II. Fig. 6 displays the variation of η, $|\zeta_1|^2$ and $|\zeta_2|^2$ according to the number of iterations N for

$f = 11.5GHz$ GHz and $\mu = 0.055$. We observe that, η, $|\zeta_1|^2$ and $|\zeta_2|^2$ simultaneously decrease with the increase in the number of iterations N. Unlike the conventional modal methods, the performances of proposed neuromodel are controlled by the operator by choosing the value of μ.This feature makes our neuromodel more versatile than the conventional modal methods. We take N=80 iterations and $\mu = 0.055$ which gives $\eta < 9.710^{-3}\%$ for all studied frequencies. Fig. 7 displays the variation of $|S_{11}|$ and $|S_{12}|$ in the considered frequency band. We observe that, the proposed neuromodel converges to the same solutions provided by the MVM and the MM. However, the proposed neuromodel is the most rapid (see table 1).

Fig. 8 displays the variation of the phases φ_{ij} of the S parameters in the considered frequency band. The solutions provided by the proposed neuromodel agree well with those produced by the modal methods.

B. E-Discontinuity

Fig. 9 displays an E-discontinuity (a=22.86 mm, b=6 mm and b'=10 mm). We take 50 modes in the waveguide I and 88 modes in the waveguide II. We set N=60 iterations and $\mu = 0.05$ which provides $\eta < 1.7210^{-3}\%$ for all considered frequencies.

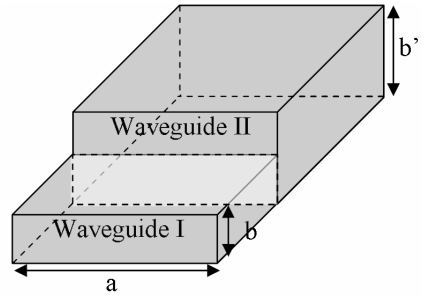

Fig. 9. E-Discontinuity

Table 2: CPU time for the studied numerical methods for the E-discontinuity

	MM	MVM	Proposed Neuromodel
CPU time (s)	3.70	3.68	3.42

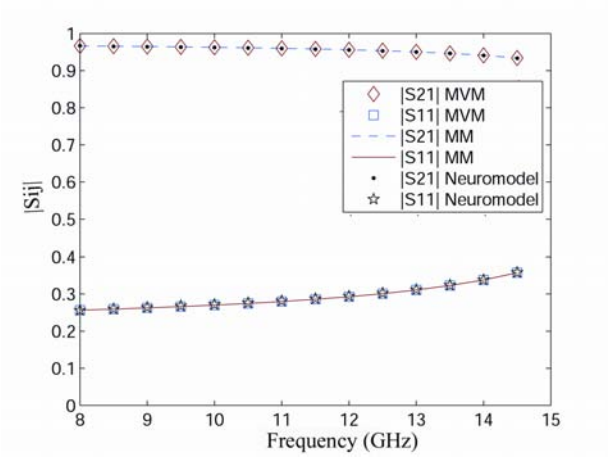

Fig. 10. $|S_{11}|$ and $|S_{12}|$ of the studied numerical methods for the E-discontinuity.

Fig. 10 displays the variation of $|S_{11}|$ and $|S_{12}|$ in the considered frequency band. We can see that all studied numerical methods converge to the same solution. However, table 2 shows that, the proposed neuromodel is the most rapid. We can obtain more rapid solutions if we take less iterations but the precision of the solution will be reduced.

C. H-Discontinuity

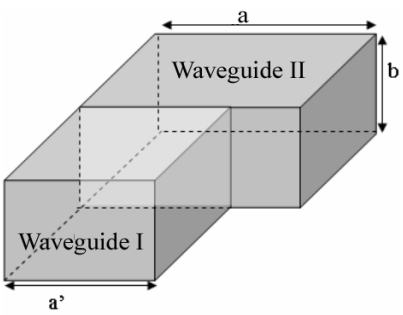

Fig. 11. H-discontinuity

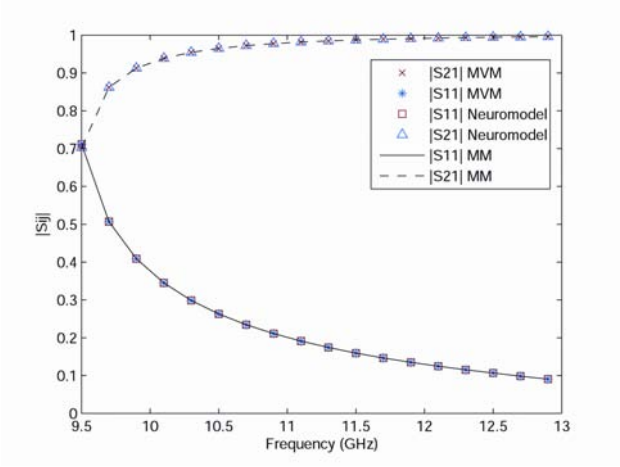

Fig. 12. $|S_{11}|$ and $|S_{12}|$ of the studied numerical methods for the H-discontinuity.

Table 3: CPU time for the studied numerical methods for the H-discontinuity.

	MM	MVM	Proposed Neuromodel
CPU time (s)	3.59	3.59	3. 55

Fig. 11 displays an H-discontinuity between two rectangular waveguides (a=22.86 mm, a'=15.9 mm and b=10.16 mm). We take 50 modes in the waveguide I and 69 modes in the waveguide II. We set N=60 iterations and μ=0.1 which provides $\eta < 3.4410^{-5}$ % for all considered frequencies.

Fig. 12 displays the variation of $|S_{11}|$ and $|S_{12}|$ in the considered frequency band. The solutions provided by the numerical methods are similar. However, table 3 shows again that the proposed neuromodel is the most rapid.

V. CONCLUSION

We proposed a hybrid neural network/modal method computer-aided design (CAD) tool to the analysis of uniaxial discontinuities in rectangular waveguides. The continuity equations of the tangential electric and magnetic fields are written in a neural model. We utilized the LMS algorithm to train the ANN weighting coefficients. The results show that the performances of the proposed neuromodel increase with the increasing of CPU time. The neuromodel is more rapid than the modal methods and provides the same accuracy.

REFERENCES

[1] C. Christodoulou and M. Georgiopoulos, "Applications of Neural Networks in Electromagnetics ", *Artech House Antennas and Propagation Library* 2001.

[2] J. E. Rayas-Sánchez, "EM-Based Optimization of Microwave Circuits Using Artificial Neural Networks: The State-of-the-Art", *IEEE Trans. Microwave Theory Tech.*, vol. 52, no. 1, pp. 420-435, 2004.

[3] P. Ramouhalli, L. Udpa and S. S. Udpa, "Finite-Element Neural Networks for Solving Differential Equations", *IEEE Trans. Microwave Theory Tech.*, vol. 16, pp 1381–1392, Nov. 2006.

[4] J. Takeuchi and Y. Kosugi, "Neural network representation of finite element method", *Neural Netw.*, 1994, 7, (2), pp. 389–395

[5] H. Yamashita, N. Kowata, V. Cingoski and K. Kaneda , "Direct solution method for finite element analysis using Hopfield neural network", *IEEE Trans. Magn.*, 1995, 31, (3), pp. 1964–1967.

[6] R. Sikora, J. Sikora, E. Cardelli and T. Chady , "Artificial neural network application for material evaluation by electromagnetic methods", IEEE *Int. Joint Conf. Neural Networks*, vol. 6, pp. 4027–4032, 1999, Washington, DC.

[7] F. Guo, P. Zhang, F. Wang and X. Guanyuanqiu, "Finite element analysis-based Hopfield neural network model for solving nonlinear electromagnetic field problems", *IEEE Int. Joint Conf. Neural Networks*, vol. 6, pp. 4399–4403, 1999, Washington, DC.

[8] M.S. Al Salameh and E.T. Al Zuraiqi, "Solutions to electromagnetic compatibility problems using artificial neural networks representation of vector finite element method", *IET Microw. Antennas Propag.*, vol. 2, no. 4, pp. 348–357, 2008.

[9] J. W. Tao and H. Baudrand, "Multimodal variational analysis of uniaxial waveguide discontinuities", *IEEE Trans. Microwave Theory Tech.*, vol. 39, no. 3, pp. 506-516, Mar. 1991.

[10] A. Wexler, "Solution of Waveguide discontinuities by Modal Analysis", *IEEE Trans. Microwave Theory Tech.*, vol. 15, pp 508 – 517, Sept. 1967.

[11] J. Jin, "The Finite Element Method in Electromagnetics", *John Wiley & sons*, Second edition, New York 2000.

[12] A. Taflove, "Computational Electromagnetics: The Finite-Difference Time-Domain Method", *Norwood, MA: Artech House*, 1995

[13] S. V. Vaseghi , "Advanced Signal Processing and Digital Reduction", *Wiley publishers* 1996 .